

# AN INTEGRATED BEAM OPTICS-NUCLEAR PROCESSES FRAMEWORK IN COSY INFINITY AND ITS APPLICATIONS TO FRIB\*

B. Erdelyi#, Northern Illinois University, DeKalb, IL 60115. and ANL, Argonne, IL 60439  
L. Bandura, NSCL, Michigan State University, East Lansing, MI 48824

## Abstract

When faced with the challenge of the design optimization of a charged particle beam system involving beam-material interactions, a framework is needed that seamlessly integrates the following tasks: 1) high order accurate and efficient beam optics, 2) a suite of codes that model the atomic and nuclear interactions between the beam and matter, and 3) the option to run many different optimization strategies at the code language level with a variety of user-defined objectives. To this end, we developed a framework in COSY Infinity with these characteristics and which can be run in two modes: map mode and a hybrid map-Monte Carlo mode. The code, its applications to the FRIB, and plans involving large-scale computing will be presented.

## INTRODUCTION

The next generation of nuclear physics research will require advanced exotic beam facilities based on heavy ion driver accelerators. There are many next-generation facilities that are currently under commissioning, construction, or envisioned [1-5]. Included amongst these is the future Facility for Rare Isotope Beams (FRIB) at the National Superconducting Cyclotron Lab at Michigan State University. These facilities are capable of producing exotic beams composed of rare nuclei in large quantities. The exotic isotopes are produced via projectile fragmentation and fission in targets. High-performance fragment separators, a key component of all rare isotope facilities, consist of superconducting magnets that are used for the capture, selection, and transport of rare isotopes. Large aperture magnets are necessary in order to accept rare isotope beams with large emittances resulting from their production mechanism.

The beam optics code COSY INFINITY uses powerful differential algebraic (DA) techniques for computing the dynamics of the beam in the fragment separator through high order transfer maps [6]. However, until now it has lacked the ability to calculate the beam-material interactions occurring in the target and energy absorbers. Here, a hybrid map-Monte Carlo code has been developed and integrated into COSY in order to calculate these interactions. The code tracks the fragmentation and fission of the beam in target and absorber material while computing energy loss and energy and angular straggling as well as charge state evolution. This is accomplished by implementing auxiliary codes such as ATIMA [7] and GLOBAL [8]. EPAX [9] is utilized to return cross

sections of fragmentation products. The special case of fission has been treated by using the code MCNPX [10] to accurately predict the cross sections and dynamics of exotic beams produced by a  $^{238}\text{U}$  beam incident on a Li or C target. The extensions to the code have made it possible to simultaneously compute high order optics and beam-material interactions in one cohesive framework.

The hybrid map-Monte Carlo code can calculate important quantities that describe the performance of the fragment separator. These include the transmission and the separation purity. In a map-only approach, calculations such as these are not possible. Experimental planning and optimization is possible with the hybrid map-Monte Carlo code, as various fragment separator settings can be readily adjusted. Here we present a description of the code, examples of calculations with it, and its application to the separation of rare isotopes.

## IMPLEMENTATION

A solely map-based approach is not sufficient to model the evolution of an exotic beam in the fragment separator. It is impossible to take into account fragmentation and fission of the beam in matter in such an approach. There are also many other effects that are nondeterministic. Stochastic effects such as energy and angular straggling in matter and charge exchange demand a Monte Carlo method. To compute the extent of the stochastic effects, the most up-to-date programs such as ATIMA for calculating energy loss and energy and angular straggling have been integrated into COSY as simple procedures.

To get an accurate view of the evolution of the beam, any material that the beam passes through must be divided up into "slices." There are a couple of reasons to do this. One reason is that some of the rarer isotopes would not be produced at all if the whole target or wedge material thicknesses were used. By the same argument, each slice cannot be too thick as it won't account for multiple fragmentations or fissions. Having slices that are too thin increases the run time of the program. Also, the data acquired from MCNPX assumes a very thin thickness ( $0.1068 \text{ g/cm}^2$ ), so any deviation from this thickness per slice will give increasingly inaccurate results. The approximation for the cross sections and dynamics will be worse. A target thickness on this order will not be used for a FRIB, so for the most accurate approximations, more than one slice per target is used. The target thicknesses would typically be about 30%-40% of the range of the primary beam in the target material. Convergence tests have been performed to determine how many slices are necessary for a normal target thickness. This value is approximately one slice per 10% of the

\*This work was supported by the U.S. Department of Energy, Office of Nuclear Physics, under Contract No. DE-AC02-06CH11357  
#erdelyi@anl.gov

projectile's range in the target material. The number of slices, however, is input by the user so more slices or fewer slices may be used. Particles are transported through the target by computing the map of each target or wedge slice and, in addition, the beam is allowed to fragment or fission only once per slice. The results of the creation of the particles in each slice, and the dynamics that occur must be composed slice by slice to get the full results of the beam's isotopic composition and dynamics for a whole target or absorber.

## RESULTS

The performance of the fragment separator can be described quantitatively by two values, namely the separation purity and transmission. These quantities can only be determined with the map-Monte Carlo code. The separation purity is key to showing how much background contamination exists at the end of a separation. The transmission indicates the ratio of the number of particles of a particular rare isotope at the end of a separation stage to the number that is formed in the target. In some cases the separation purity may be good but the transmission is poor or vice versa. The two quantities must be evaluated together to effectively evaluate the performance of the separator.

In addition to having a desirable separation purity and transmission, it is also necessary that in some cases that all of the particles of the separated rare isotope beam have the same energy. In cases such as these, additional optics and a properly shaped energy absorber must be used to achieve a monochromatic beam.

### Transmission

There are four general reaction mechanisms that take place when the primary beam interacts with a target. These include light and heavy nuclear fragmentation and light and heavy nuclear fission. The transmissions of isotopes produced by these mechanisms are shown in Table 1. The transmissions were calculated for a target thickness of 20% of the range of the primary beam in a Li target and wedge thicknesses of 30% of the range of the selected isotope beam energy in a two-stage separator.

Table 1: Transmissions According to Production Mechanism

Production Mechanism	Isotope	Transmission (%)
Light Fragmentation	<sup>14</sup> Be	90.6
Heavy Fragmentation	<sup>100</sup> Sn	91.0
Light Fission	<sup>78</sup> Ni	21.5
Heavy Fission	<sup>132</sup> Sn	42.9

There is a great dependence of the transmission on the reaction mechanism which produces each isotope. The best transmission results from fragmentation due to the low initial emittance of the rare isotope beam. The transmission is lower for fission products as they are initially emitted from the target with large angular and energy spread. This causes the loss of the isotope since it travels beyond the apertures of the fragment separator.

Due to the challenges of fission products in particular, a comprehensive transmission study was conducted for the fission product <sup>132</sup>Sn. This isotope was chosen for its importance to the nuclear physics community and the fact that a beam of <sup>132</sup>Sn has a large emittance and, hence, is one of the most difficult to capture. For this study, a 200 MeV/u <sup>238</sup>U beam is incident on a Li target of variable thickness. It fissions, producing <sup>132</sup>Sn among thousands of other isotopes. The thicknesses of the target and the first and second wedges of a two-stage separator are varied in increments of 10% of the range of <sup>238</sup>U in a Li target and <sup>132</sup>Sn in the two Al wedges for all thickness combinations between 10% and 60% of the range for the target thickness and 10% and 70% of the range for the wedges. The transmission of <sup>132</sup>Sn after two separation stages is shown in Figure 1 for constant target thickness and varied wedge thicknesses. While it is obvious that with increasing material in the system the transmission decreases, the transmission depends slightly more on the first wedge thickness than the second. This difference is more pronounced for thin targets.

### Separation Purity

The separation purity,  $\phi$ , describes the fragment separator's ability to select one isotope from all

others:  $\phi = \frac{N_{A_0, Z_0}}{N_{A, Z}}$ , where  $N_{A_0, Z_0}$  is the total number of

particles of the separated isotope at the end of a separation stage.  $N_{A_0, Z_0}$  is the total number of particles of all isotopes at the end of a separation stage.

This quantity depends on many things which are not explicit in this expression. First, the optics of a fragment separator system must be optimal to focus the separated isotope in as small as a region in  $x$  as possible. The ability to do this differs according to the isotope and the reaction mechanism by which it is produced. The primary beam also plays a role in producing the type and quantity of background impurities that exist in the system. If the primary beam is of low  $Z$ , the background impurities must have equal or lower  $Z$  and the contamination will be low to insignificant. If, however, a high  $Z$  beam such as <sup>238</sup>U is used, the range of contaminating isotopes produced is vast. Also, a radioactive beam such as this will produce background that would not otherwise be seen with a beam that is produced solely by fragmentation. The addition of fission as a production mechanism leads to an even broader range of isotopes produced and, in addition, these production rates are dependent on the energy of the primary beam.

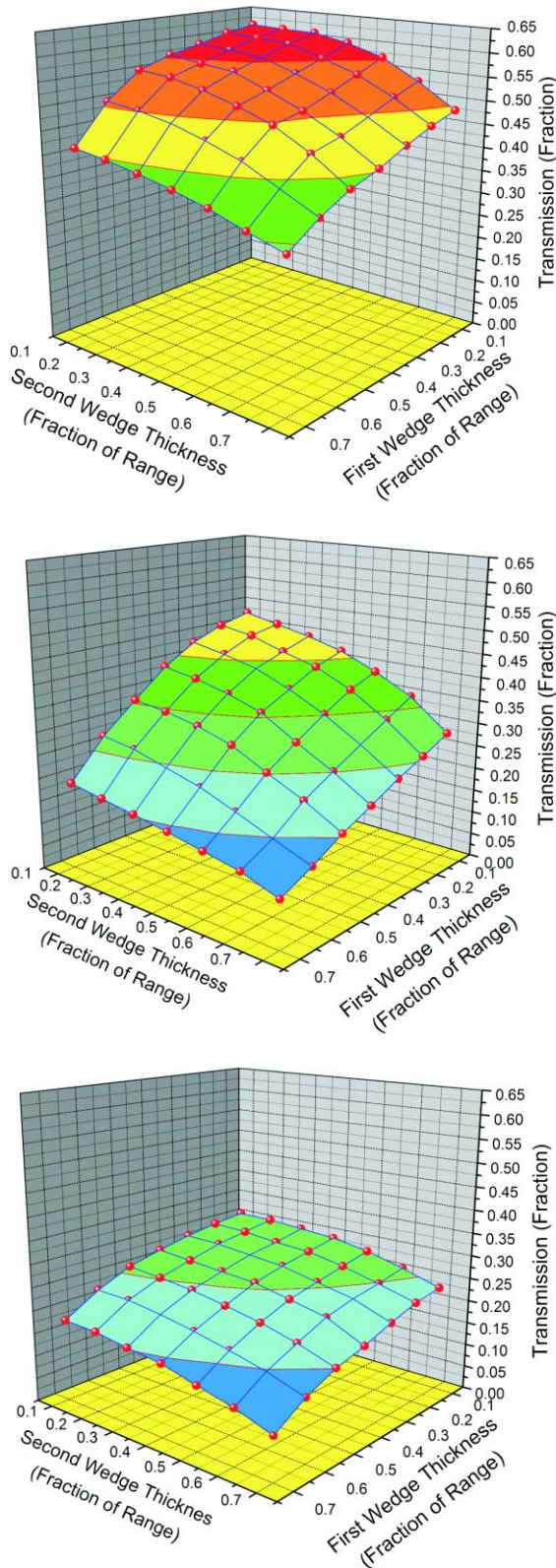


Figure 1: Transmission as a function of first and second wedge thicknesses in a two-stage separator. Target thicknesses are 10, 30, and 50% of the primary beam’s range in target material (from top).

There are four general production mechanisms that have different beam dynamics and background that either complicate or make the separation easier. These mechanisms represent the extremes of the dynamics in the separator. All other isotope production mechanisms fall between these extremes in beam dynamics. For each of these four reaction mechanisms, one isotope was selected to be studied in detail. In each of these cases, the energy of the beam is limited by the parameters of the FRIB linear accelerator. The maximum energy that a primary beam attains is  $^{238}\text{U}$  accelerated to 200 MeV/u. The optimal target and wedge thicknesses in each case are computed using the program LISE++ [11].

The optimization is completed for a one stage separation; the second stage has the same wedge thickness in terms of fraction of the range of the rare isotope beam in Al.

The separation purity of many rare isotopes has been calculated for four types of production mechanisms representing the extremes in beam dynamics (Table 2). The results yielded 100% purity for a one stage separation of  $^{14}\text{Be}$ , a light fragmentation product. For  $^{100}\text{Sn}$  (Figure 2), the separation purity is 7.5% after two separation stages, with only one contaminant. The heavy fission product,  $^{132}\text{Sn}$ , has a separation purity of 4.04% after two stages. The light fission product,  $^{78}\text{Ni}$  is challenging to separate with a separation purity of only 0.003% after two separation stages. Separation purity with the gas cell branch has also been computed for each of these isotopes.

Table 2: Separation Purity According to Production Mechanism

Production Mechanism	Isotope	One Stage	Two Stage	Gas Cell Branch
		$\phi$ (%)	$\phi$ (%)	$\phi$ (%)
Light Fragmentation	$^{14}\text{Be}$	100	100	96.7
Heavy Fragmentation	$^{100}\text{Sn}$	$7.73 \times 10^{-5}$	$5.89 \times 10^{-2}$	$1.48 \times 10^{-3}$
Light Fission	$^{78}\text{Ni}$	$2.79 \times 10^{-2}$	0.364	$2.94 \times 10^{-2}$
Heavy Fission	$^{132}\text{Sn}$	1.15	4.04	1.52



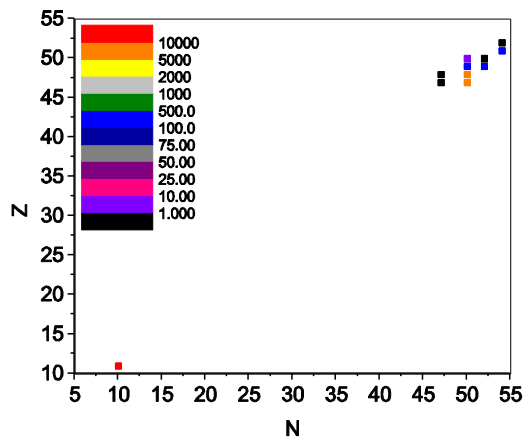


Figure 2: Distribution of isotopes that remain after the one stage separation of  $^{100}\text{Sn}$ . Remaining isotopes are plotted in the N-Z plane. The quantities of the isotopes at the end of the system are indicated by the color of the box with all isotope quantities scaled such that one  $^{100}\text{Sn}$  particle is at the end of the separation stage.

## GAS CELL BRANCH

ISOL (Isotope Separation On Line) is not sufficient to study some isotopes. These isotopes need to be studied at a lower energy, and therefore are stopped in a neutral He gas cell. This low-energy regime is key for many nuclear physics and astrophysics experiments. For these cases, the second separation stage of a two-stage fragment separator is replaced with a monochromatic gas cell branch. This is necessary in order to stop all of the particles selected in the separation in as small of a region as possible in the He gas cell. In some cases, after stopping the isotopes in the gas cell, they may be reaccelerated to the desired energy. After the achromatic image of the first stage, the optics of the first half of the first stage are repeated, followed by a monochromatic wedge. A monochromatic absorber is obtained by shaping the wedge to cancel the wedge map element  $(\delta|\delta)$  at first order and potentially further shaping it to cancel the map aberrations  $(\delta|\delta^n)\delta_i^n$ , where n is the order of the aberration.

## CONCLUSION

A hybrid map-Monte Carlo code has been developed to accurately model beam-material interactions for the purpose of fragment separator beam dynamics simulations. This code has allowed for the calculation of important quantities that determine quality of the separation. These include the transmission and separation purity. Using the code, one may simulate a variety of exotic beam experiments. Future work will focus on more detailed optimization to find the best fragment separator settings for rare isotopes to be captured for experiment.

[Computer Codes \(Design, Simulation, Field Calculation\)](#)

## REFERENCES

- [1] RISAC. Scientific Opportunities with a Rare-Isotope Facility in the United States. Technical report, NRC, 2006.
- [2] J. Nolen. Overview of the U.S. Rare Isotope Accelerator Proposal. Nucl. Phys., A734:661.668, 2004.
- [3] Y. Yano. RI Beam Factory project at RIKEN. In Proc. 17th Int. Conf. Cycl. Appl., pages 169.173, Tokyo, Japan, 2004.
- [4] T. Kubo, K. Kuska, and K. Yoshida et al. Status and overview of superconducting radioactive isotope beam separator BigRIPS at RIKEN. IEEE Transactions on Applied Superconductivity, 17:1069.1077, 2007.
- [5] W. Henning. The GSI project: An International Facility for Ions and Antiprotons. Nucl. Phys., A734:654.660, 2004.
- [6] M. Berz. Modern Map Methods in Particle Beam Physics. Academic Press, San Diego, 1999.
- [7] H. Weick. <http://www-linux.gsi.de/weick/atima/>.
- [8] C. Scheidenberger, T. Stohlker, W. Meyerhof, H. Geissel, P. Mokler, and B. Blank. Charge states of relativistic heavy ions in matter. NIM B, 142:441.462, 1998.
- [9] K. Summerer and B. Blank. EPAX version 2: a modified empirical parameterization of fragmentation cross sections. Nuclear Physics A, 701:161C.164C, 2002.
- [10] M. James, G. McKinney, J. Hendricks, and M. Moyers. Recent enhancements in mcnpx: Heavy-ion transport and the LAQGSM physics model. NIM A, 562(2):819.822, 2006.
- [11] O. Tarasov and D. Bazin. LISE++: design your own spectrometer. Nuclear Physics A, 746:411.414, 2004.